

1 Multi-Faceted Framework for Extrapolating Early Age Flexural Strength to
2 Facilitate Rapid Lifting/Handling of High-Volume Fly Ash Precast Members

3 Zoe N. Lallas^a, Matthew J. Gombeda^b, and Kurt A. Ordillas^c

4 **ABSTRACT**

5 Maintaining adequate early-age structural performance for precast concrete components
6 has grown in importance as more sustainable mix designs become more widespread. Achieving
7 high-early flexural strength is particularly crucial to facilitate rapid removal of hardened concrete
8 components from formwork, often within twenty-four hours after fresh concrete placement.
9 Limited research has assessed the effectiveness of traditional design methods in correlating
10 flexural strength with compressive strength for next-generation mix designs, or demonstrated
11 extrapolation of such material performance to larger-scale structural tests. This paper presents a
12 multi-faceted framework to reassess early-age flexural strength for concretes made with relatively
13 high proportions of fly ash from both fresh and harvested sources. The framework provides several
14 pathways, from which the user can select based upon available resources and the specific
15 application, to improve accuracy of early-age cracking moment calculations. Furthermore, the
16 scope includes evaluation of strength performance under curing conditions emulative of those in a
17 precast facility, recommending modulus of rupture equations which are more performance-driven
18 than current design provisions, and experimental tests on prefabricated concrete beams to validate
19 the proposed methodologies. Correlations of early-age strength with both concrete age and
20 maturity measurements compare the effectiveness of utilizing in-situ data to further enhance the

^a Graduate Research Assistant, Department of Civil, Architectural and Environmental Engineering, Illinois Institute of Technology, 3201 S. Dearborn St., Chicago, IL USA 60616. Email: zlallas@hawk.iit.edu. **Corresponding Author.**

^b Assistant Professor of Civil Engineering, Department of Civil, Architectural and Environmental Engineering, Illinois Institute of Technology, 3201 S. Dearborn St., Chicago, IL USA 60616. Email: mgombeda@iit.edu

^c Former Graduate Research Assistant, Department of Civil, Architectural and Environmental Engineering, Illinois Institute of Technology, 3201 S. Dearborn St., Chicago, IL USA 60616. Email: kurtordillas@gmail.com

21 prediction methods. Ultimately, the proposed framework helped reduce errors when calculating
22 cracking moment capacity at early ages by tailoring calculations to reflect mix-dependent
23 behavior. Furthermore, most estimates of cracking moment were within 25% of their
24 corresponding experimental test results, thus promoting confidence for using these strategies with
25 high-volume fly ash precast structures.

26 **Keywords:** Precast, Fly Ash, Early-Age, Rupture, Cracking

27 **1. INTRODUCTION**

28 The use of supplementary cementitious materials (SCMs) in mix designs for prefabricated
29 concrete components is becoming more widespread due to increasingly stringent restrictions for
30 energy efficiency or carbon emissions during production of conventional Portland cement
31 products. Fly ash has a longstanding history of beneficial use in concrete mixtures, however, due
32 to its reduced heat of hydration, it can delay strength development, especially during the early-age
33 window. Therefore, increased use of fly ash for concrete products like bricks [1], cast-in-place
34 applications, or for nonstructural use [2] may have less barriers since the mechanical stresses
35 experienced in these products during the fabrication phase are generally not substantial. Precast
36 concrete components generally require rapid strength development during the initial fabrication
37 and handling phase and thus traditionally have been the recipient of more strict limitations for fly
38 ash use.

39 **1.1. *Motivation and Significance of Early-Age Flexural Strength for Precast***

40 Development of high early flexural strength is of paramount importance during the
41 fabrication of precast concrete components as this metric generally facilitates rapid removal of
42 hardened concrete members from reusable formwork and thus helps optimize the efficiency of a
43 precast facility. The design of many precast components calls for them to remain uncracked during

44 lifting/handling and therefore the allowable flexural strength of the concrete must safely exceed
45 the maximum tensile stress expected in the member at this stage, which often occurs within 24
46 hours after fresh concrete placement. The main design parameter used in the assessment of these
47 objectives is the cracking moment (M_{cr}), which is computed as a function of the plain concrete
48 modulus of rupture (f_r), the gross moment of inertia of the cross-section (I_g), and the distance from
49 the neutral axis of the cross-section to extreme tension fiber (y_t), where cracking is expected to
50 initiate. The mathematical expression for M_{cr} is shown in Equation 1 and f_r is calculated using a
51 relationship with the corresponding compressive strength (f_{cm}), usually in accordance with ACI
52 318-19 [3] Equation 19.2.3.1 (see Equation 2 in this paper where strength units are in MPa and λ
53 is a lightweight concrete factor taken as 1.0 for normalweight concrete for the purposes of this
54 study), or via direct testing of unreinforced concrete beam specimens in accordance with ASTM
55 C78 [4]. Since the former method relies on a fit equation based on the results of numerous
56 experimental studies with varying types of concretes [5], it is generally recommended to reexamine
57 the effectiveness of such an equation when new variations of mix formulations are evaluated.
58 Furthermore, these conventional design equations were not developed specifically for the purpose
59 of assessing the early-age performance of concretes with relatively high portland cement
60 replacement fractions – as will be a major underlying focus of this study. Traditionally,
61 incorporating larger fractions of fly ash in concrete mix designs results in lower heat of hydration
62 of the binder matrix and consequently can delay the development of compressive or tensile
63 strength of a hardened concrete specimen. Therefore, it is imperative to first demonstrate the
64 scalability of the mechanical performance observed when testing high-volume fly ash (HVFA)
65 concrete specimens up to larger-scale fabrication and testing of HVFA beams. Secondly, it is
66 equally important to reassess the procedure for calculating early-age flexural strength to ensure the

67 inherent mechanics of the novel mix designs are reflected in current design provisions or to
68 recognize where modifications to such provisions may be needed in such cases moving forward.

$$M_{cr} = \frac{f_r I_g}{y_t} \quad \text{Equation 1}$$

$$f_r = 0.623\lambda\sqrt{f_{cm}} \quad \text{Equation 2}$$

69 In addition to its constituents, curing conditions – namely temperature and humidity – can
70 significantly affect strength development of a given concrete mix, especially for applications
71 where ambient conditions (i.e., uncontrolled temperature and humidity) are present during the
72 curing process as is common in many precast facilities. Therefore, providing ambient conditions
73 in the laboratory which emulate those expected under normal precast fabrication operations is
74 critical to streamlining the scalability of the mechanical properties garnered from HVFA cylinders
75 and small plain beams up to the corresponding performance of larger-sized HVFA beams or other
76 types of precast components. Based on the aforementioned rationale, this paper presents a multi-
77 faceted framework designed to streamline and customize the calculation of the early-age flexural
78 strength of a structural concrete member fabricated with high-volume fly ash (including harvested
79 or landfilled fly ashes) concretes. More specifically, the framework consists of three tracks, each
80 with varying combinations of complexity and accuracy with respect to test results, that can be used
81 to calculate the cracking moment. The first track is the most similar to conventional methods using
82 a correlation between the modulus of rupture and the square root of the corresponding compressive
83 strength, albeit with proposed modifications to the equation coefficients to more accurately capture
84 the early-age behavior of novel HVFA mixes. The second track employs a maturity-based
85 approach which correlates temperatures in HVFA concrete beams back to temperatures recorded
86 during mechanical testing of small specimens (i.e., cylinders and small plain concrete beams)
87 prepared with the same mix formulation to assist in generating strength development histories.

88 Lastly, the third track is based on direct modulus of rupture testing to calculate cracking moment
89 and will largely be used for comparison with the other two tracks as it is theoretically the most
90 straightforward and least reliant on statistical analyses – assuming the user has the proper
91 equipment to perform this type of test. Several rounds of preliminary experimental testing of
92 hardened HVFA concrete specimens under ambient curing conditions will influence slight
93 modifications to conventional design equations for modulus of rupture as needed. Lastly, a series
94 of larger-scale experimental tests on prefabricated HVFA concrete beams performed within 24
95 hours after fresh concrete placement will demonstrate the effectiveness of the proposed framework
96 in estimating the cracking moment.

97 ***1.2. Influence of Concrete Maturity when Assessing Strength Development***

98 Concrete maturity is defined as the area under the temperature-time history of a given
99 concrete sample, ranging from the time of concrete placement to a given time of interest for
100 estimating the strength of the mix. The maturity approach is commonly used to monitor the internal
101 temperature of curing concrete and subsequently calculate the expected strength (e.g.,
102 compressive, flexural, etc.) by correlating the temperature reading back to a strength-maturation
103 curve originally developed during mix trials in the laboratory. Noteworthy benefits of this
104 approach are twofold, first is that the internal temperature of the member can be influenced by
105 curing conditions and a relatively slow or faster curing regimen is more likely to be accounted for
106 when estimating hardened concrete strength. Secondly, the use of maturity curves facilitates a non-
107 destructive means of approximating in-situ concrete strength as it only requires a temperature
108 sensor and does not necessitate costly or infeasible core samples to be extracted from the member
109 as part of an in-situ evaluation.

110 A simple means to calculate concrete maturity, M , uses the Nurse-Saul function where the
111 relationships between maturity and both age and temperature are assumed to be linear [6] as shown
112 in Equation 3 where t is the age of the concrete (the time of placement is zero and the desired time
113 at which to calculate maturity is t_f), T is the instantaneous temperature in the concrete, and T_0 is
114 the datum temperature. Currently, there exist means of monitoring the maturity of in-situ concrete
115 computationally with a remote temperature sensor and computer interface where mix proportions
116 can be uploaded and maturity is determined based upon the Nurse-Saul method and current
117 standards including ASTM C1074 [7], ASTM C918 [8], and ACI 318 [3]. Integrated calculation
118 of maturity based on wireless continuous temperature monitoring streamlines maturity
119 determination for novel mix designs, particularly those containing SCMs [9].

$$M = \sum_{t=0}^{t=t_f} (T - T_0) * \Delta t \quad \text{Equation 3}$$

120 When originally proposed, concrete maturity was thought to manifest independent of
121 curing conditions, but this hypothesis has since been disproven in literature [6,10–13]. It also does
122 not account for the impact curing conditions have on the instantaneous temperature of the concrete
123 (i.e. concrete cured outside, while generating the same amount of heat as concrete cured indoors,
124 can lose significantly more heat to the ambient air). While instantaneous maturity can be
125 considered independent of curing conditions, the rate at which maturity develops is heavily
126 impacted by the surrounding curing environment. Although temperature fluctuations are often less
127 of a concern for precast components fabricated under plant conditions (relative to cast-in-place
128 construction), many precast facilities are not completely climate controlled and thus emulating the
129 expected conditions in the factory is likely to produce the most accurate correlations between
130 strength development and the maturity readings taken from a precast component when curing.

131 Geng et al. [6] found the Nurse-Saul method to be less accurate in environments where high
132 temperature fluctuations are common, such as outdoors, and the relationship between recorded
133 temperature and maturity may no longer be linear in such cases. Kanavaris and Soutsos [14] found
134 that, in general, the Nurse-Saul equation will lead to a conservative estimate of strength,
135 particularly at early ages and in the presence of heat curing. Their work resulted in a modified
136 Nurse-Saul method to iteratively determine strength. Recognizing that maturity in the first 24
137 hours is often the most difficult to determine, Hrishev et al. [15] monitored temperature at two
138 depths in their 50 x 50 x 25 cm concrete specimen and determined maturity using the Nurse-Saul
139 method. Strength was tested at 1, 3, 7, 14, and 28 days, and determined as a logarithmic function
140 of maturity. The calculated compressive strength was within 15% for concrete tested at 3 days and
141 beyond, but their models were less accurate prior to 3 days [15], most likely because concrete
142 curing conditions play a vital role in determining early age strength (and maturity). Kazemifard et
143 al. [16] also determined compressive strength as a logarithmic function of maturity and, on
144 average, their approach yielded 94% accuracy to compressive strength determined via destructive
145 testing.

146 The equivalent age method was established for determining maturity in concrete cured in
147 environments where temperature and maturity are not directly proportional (outside of 0-40°C)
148 and instead involves finding an equivalent age of the concrete based on an exponential function of
149 the instantaneous internal temperature [9]. The maturity method outlined in ASTM C1074 [7] is
150 well established for determining concrete age beyond 24 hours, and the framework herein follows
151 a similar approach with an emphasis within the 24 hour age period. Literature supports a
152 logarithmic relationship between maturity and strength [11,12,15–17] which commonly follows
153 the format shown in Equation 4 where S is the strength (compressive, rupture, or other), M is the

154 maturity of the concrete, determined manually pursuant to ASTM C1074 [7] or computationally
155 using integrated software, X may be any base – but most commonly 10 or e – and a and b are mix-
156 dependent constants, which are determined through destructive testing and regression analysis of
157 the time- or maturity-dependent strength values.

$$S = a + b * \log_X M \quad \text{Equation 4}$$

158 **1.3. *Influence of Curing Conditions***

159 For the purposes of this study, temperature- and/or moisture-controlled curing
160 environments will refer to the conditions found in a laboratory-type environmental chamber or
161 other apparatus designed to allow concrete specimens to develop strength under ideal temperature
162 and humidity. Contrarily, ambient curing will refer to open-air conditions of a laboratory setting
163 or a precast facility, without close regulation of temperature and humidity. Heat produced during
164 concrete curing (the result of the hydration of cementitious materials) does not develop as rapidly
165 in temperature- and moisture-controlled environments, as is common in laboratory settings and
166 curing chambers designed specifically to control these variables. Heat curing can also increase the
167 rate at which maturity develops compared to both temperature- and moisture-controlled curing
168 (i.e. curing chambers) and ambient curing. In extreme weather conditions, maturity has been
169 shown to be a better indicator of early-age strength than time [12]. Tekle et al. [12] also found that
170 the effect of extreme cold environments on compressive strength development is not solely
171 proportional to the maturity parameter. At the same maturity, concrete cured in cold weather
172 environments achieved lower strength than concrete cured in more temperate environments,
173 further enforcing the conclusion that the Nurse-Saul method is not accurate for nonlinear
174 (irregular) maturity development. This concept generally applies to a range of curing
175 environments; for example, it can be expected that concrete cured in heated environments will

176 achieve higher early-age strengths than conventionally cured (ambient or temperature- and
177 moisture-controlled) concrete at the same maturity.

178 Ambient curing conditions, like those of cast-in-place or some large-scale precast facilities,
179 mean that the instantaneous temperature in the concrete is subject to fluctuations that will
180 inevitably occur over the curing cycle. Certain curing environments can maintain specific
181 temperatures and/or moisture levels to ensure optimal curing conditions in closed environments,
182 such as in environmental chambers. Temperature and humidity chambers ensure that the curing
183 environment remains consistent, or otherwise controlled over time. Maintaining consistent
184 temperature conditions yields slowed maturity development, which may lead to delayed strength
185 development as this is linked to the curing process. Curing chambers also help to ensure the
186 relationship between temperature and maturity remains linear by limiting temperature fluctuations
187 [6]. Better approximations of maturity and the corresponding strength performance allow for more
188 informed timing of strength-dependent construction processes [13]. Idealized conditions, like
189 those present in a curing chamber, are not guaranteed in most batching scenarios, and the
190 repeatability of ideal conditions should not be assumed. Thus, it is important to know the direct
191 impacts of curing temperature on maturity (and analogously, strength) development. Under the
192 scope of this research, maturity under ambient curing conditions was observed, and the
193 corresponding strength was recorded as a function of maturity between concrete ages of 12 and 24
194 hours. In general, it was found that under ideal curing conditions, notably 23°C (73.4°F), 95%
195 humidity in the context of concrete specimens [18], maturity develops proportionality to curing
196 environment temperature whereas in ambient warm weather conditions (particularly, 25°C (77°F),
197 50% humidity as found in the lab set up for testing purposes in this research), maturity
198 development was more accelerated relative to the ambient temperature.

199 **2. STRENGTH DEVELOPMENT BEHAVIOR**

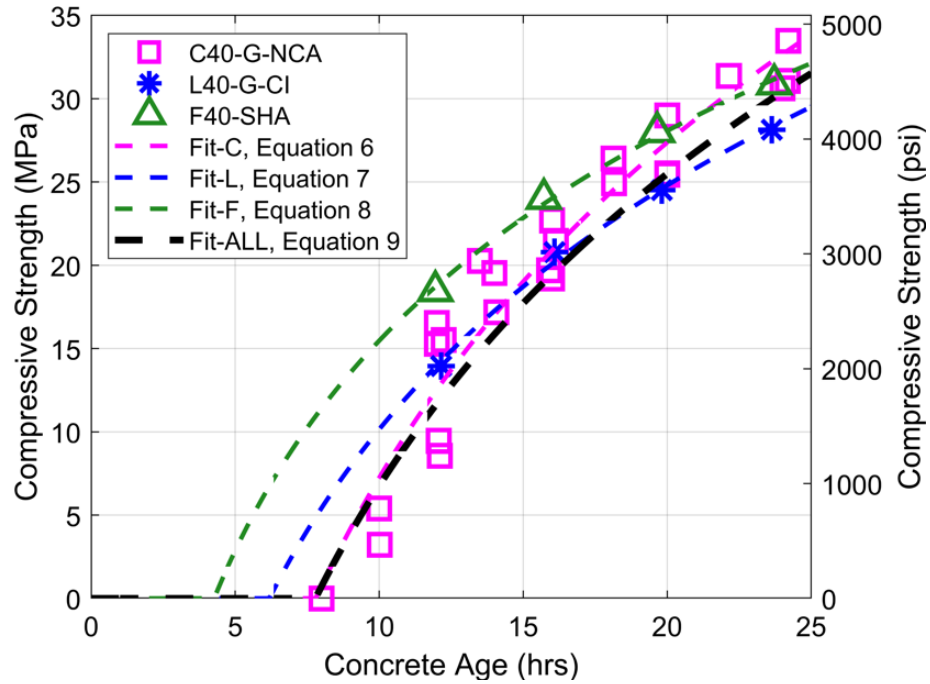
200 A critical preliminary step in advance of deploying the framework is to assess the early-
201 age strength development behavior of a given HVFA mix design in the relevant environment of
202 its intended application. Previous research by the authors [19] presented a methodology to
203 characterize the early-age strength development of novel HVFA mixes, albeit under temperature-
204 and humidity-controlled curing conditions in an environmental chamber. To increase the
205 effectiveness of that procedure for the purposes of calculating the early-age flexural capacity of a
206 precast component, this paper presents two extensions of that original work. The first subjects the
207 novel HVFA concretes to a curing environment that emulates the ambient conditions generally
208 found in a precast facility to facilitate more accurate flexural strength prediction under the
209 influence of the relevant temperature and humidity. The second adds concrete maturity as an
210 auxiliary baseline, in addition to concrete age, for which to characterize concrete compressive and
211 flexural strength against. Generally, time-based methods are recommended when curing
212 conditions will not vary between batches (like indoors, or in temperature- and humidity- controlled
213 environments) whereas the maturity-based approach may be better suited for curing environments
214 where temperature and humidity may vary between batches (such as outdoors). To generate
215 strength development curves to reflect these two objectives, a series of additional experimental
216 tests were conducted using the best performing HVFA mix design from each group of fresh Class
217 C (*C40-G-NCA*), fresh Class F (*F40-SHA*), and a harvested Class F fly ash (*L40-G-CI*) as
218 documented in Ordillas et al. [19]. During this study, compressive testing pursuant to ASTM C39
219 [20] and subsequent characterization of compressive strength relative to time or maturity was
220 conducted within 24 hours of fresh concrete batching and specimen preparation. From plots of
221 time-dependent strength, a straightforward regression analysis was used to obtain a logarithmic

222 relationship for compressive strength as a function of concrete age, t , as show in Equation 5
223 pursuant to supporting literature [11,12,15–17] where a and b are mix-dependent constants.

$$f_{cm} = a + b * \log_{10} t \quad \text{Equation 5}$$

224 These constants will change for a given mix and care should be taken to maintain curing
225 conditions during subsequent concrete production to ensure the best estimate of time-dependent
226 strength. Using time as the independent variable simplifies determination of strength when
227 compared to ASTM C1074 [7] if it is not feasible to monitor maturity for a given concrete member.
228 For each fly ash type (Class C, Class F, and harvested), compressive strength was determined
229 pursuant to ASTM C39 [20] and modulus of rupture was assessed in accordance with ASTM C78
230 [4] at ages of 12, 16, 20, and 24 hours. Maturity was also recorded at the time of each specimen
231 test using a wireless temperature sensor placed in an extra concrete cylinder. Compressive and
232 rupture strength data were then compiled, and these values were then used to determine an overall
233 HVFA strength approximation equation with respect to time and maturity, as well as mix-
234 dependent equations for each different fly ash type. Figure 1 presents compressive strength as a
235 function of concrete age, Figure 2 shows compressive strength as a function of concrete maturity,
236 and Figure 3 shows modulus of rupture as a function of compressive strength. The corresponding
237 fit equations (taking the form shown in Equation 5) for Figure 1, 2, and 3 are Equation 6-9, 10-13,
238 and 14-17, respectively, where the unit of strength is MPa, time is in hours, and maturity is in °C-
239 hrs (note that λ was taken as 1.0 in every case due to the uniform use of normalweight concrete).
240 Although the behavior of each HVFA mix design was assessed separately, general equations (see
241 Equation 9, 13 and 17) were also proposed as average fitting functions across the three separate
242 40% HVFA mixes examined in this study. Please note that the calculated compressive strength
243 must be greater than or equal to zero at any given age since the fitting equations herein were

244 adjusted to capture the best form of the data considering the effect of concrete setting time which
245 manifests as an offset to when significant strength development commences.

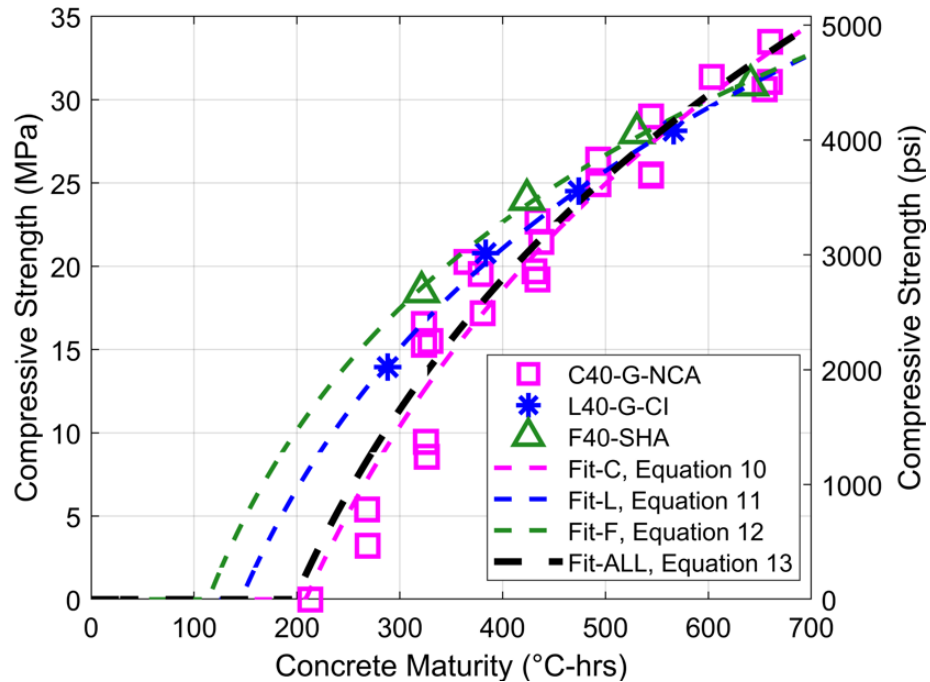


$$f_{cm} = \max (66.88 \log t - 59.64, 0) \quad \text{Equation 6}$$

$$f_{cm} = \max (48.66 \log t - 38.51, 0) \quad \text{Equation 7}$$

$$f_{cm} = \max (41.86 \log t - 26.39, 0) \quad \text{Equation 8}$$

$$f_{cm} = \max (62.22 \log t - 55.46, 0) \quad \text{Equation 9}$$



248

249 Figure 2 – Early-age compressive strength versus concrete maturity for HVFA mix designs

250

$$f_{cm} = \max (9524 \log M - 22086, 0) \quad \text{Equation 10}$$

$$f_{cm} = \max (6958 \log M - 15049, 0) \quad \text{Equation 11}$$

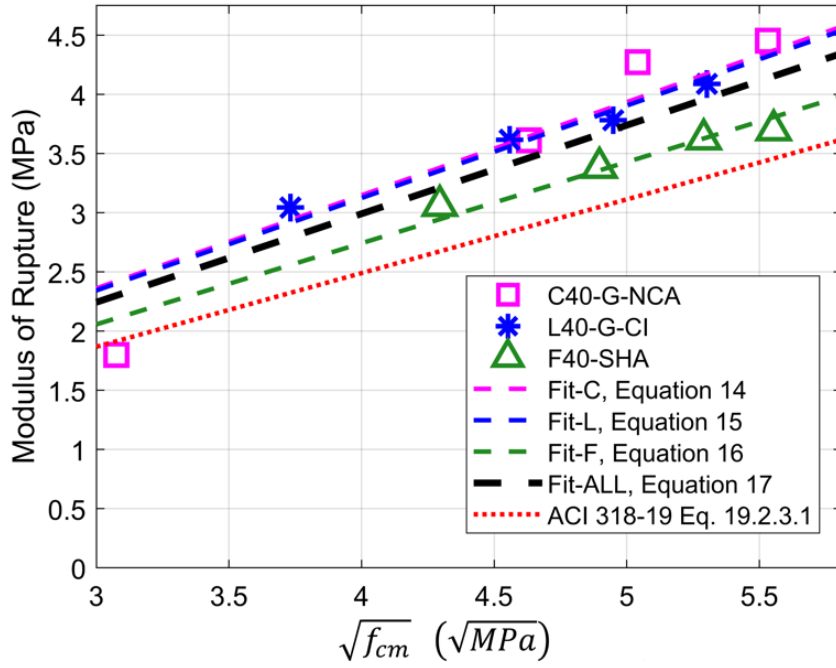
$$f_{cm} = \max (6022 \log M - 12383, 0) \quad \text{Equation 12}$$

$$f_{cm} = \max (9107 \log M - 20907, 0) \quad \text{Equation 13}$$

251

252 While Equation 2 is generally conservative for the mix formulations shown in Figure 3,
 253 developing more performance-driven equations to represent modulus of rupture can further

254 optimize precast casting bed turnover as the behavior (with respect to the standard design equation)
 255 may be deemed overly conservative for certain applications.



256
 257 Figure 3 – Characterization of early-age modulus of rupture test results as a function of the
 258 corresponding compressive strength results
 259

$$f_r = 0.787\sqrt{f_{cm}} \quad \text{Equation 14}$$

$$f_r = 0.781\sqrt{f_{cm}} \quad \text{Equation 15}$$

$$f_r = 0.686\sqrt{f_{cm}} \quad \text{Equation 16}$$

$$f_r = 0.748\sqrt{f_{cm}} \quad \text{Equation 17}$$

260 3. PROPOSED EARLY-AGE CRACKING MOMENT FRAMEWORK

261 The proposed framework aims to provide a thorough means of optimizing cracking
 262 moment approximations pursuant to the capabilities of the user; Thread I provides an estimate of

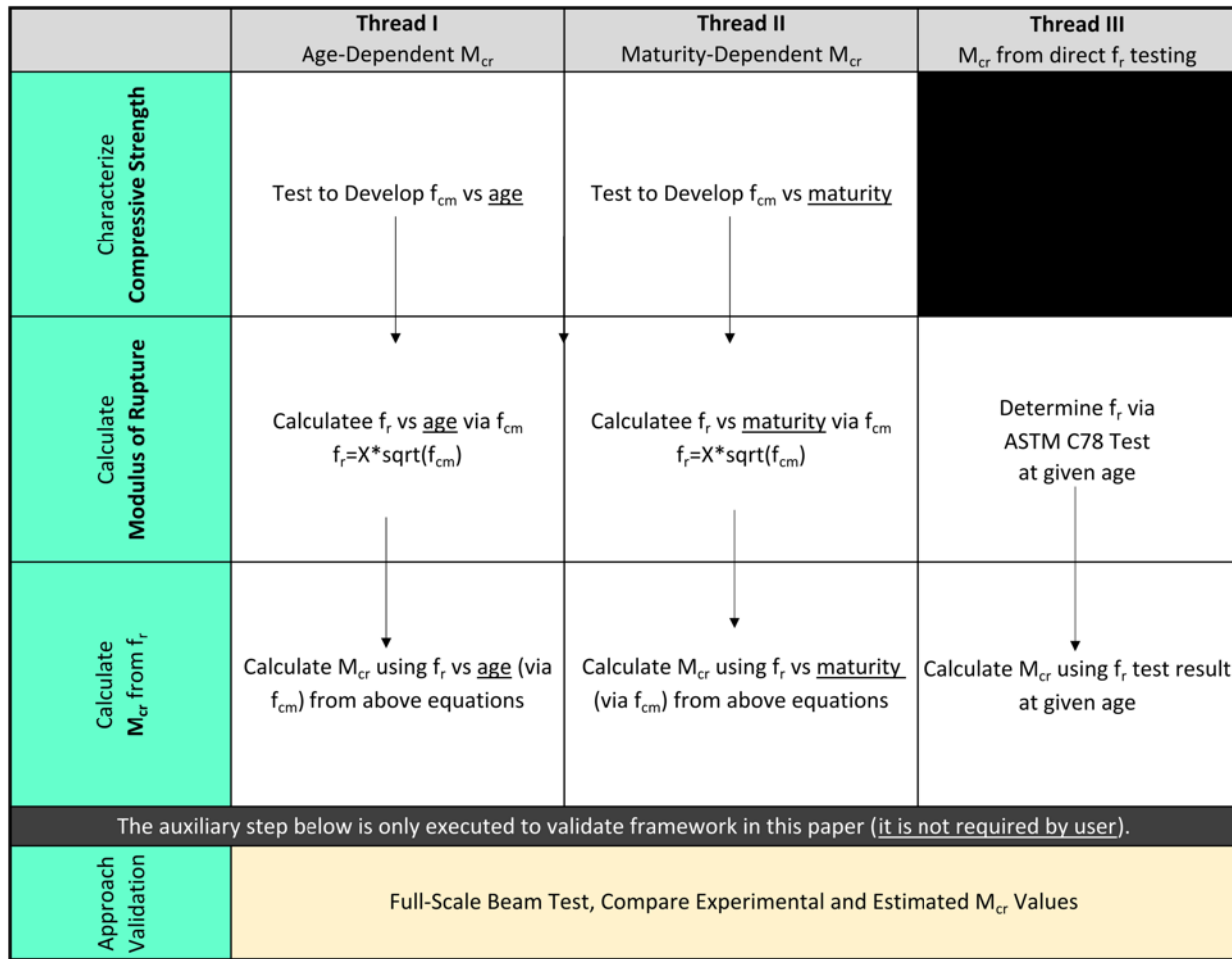
263 strength based upon concrete age and can be used in environments where curing conditions
264 generally do not fluctuate between batches, or if means of determining maturity are not feasible.
265 This estimate can be taken as an improvement relative to the currently accepted means of
266 determining strength as Thread I accounts for mix-specific strength development rather than an
267 average of historical concrete strength values. Thread II provides the advantage of accounting for
268 the impact curing environment (namely temperature and humidity) has on strength development.
269 This estimate is recommended in environments where curing conditions are expected to vary
270 significantly between batches, and is expected to provide a more informed estimate of strength
271 development than Thread I. Threads I and II have the benefit of requiring compressive testing of
272 cylinders without any additional flexural testing or specimen batching, should this be a
273 consideration at the discretion of the user. Thread III provides a more direct estimate of cracking
274 moment based upon age-dependent flexural strength obtained from testing pursuant to ASTM C78
275 [4]. This particular approach requires less statistical analyses, but necessitates casting of
276 unreinforced flexural beams and the utilization of 4-point flexural testing for determination of f_r
277 rather than calculation from the relationship between f_{cm} and f_r as described in Equation 14-
278 Equation 17.

279 For the purposes of the framework presented herein, compressive strength development
280 can first be characterized as a function of time or maturity. Thus, upon establishing an approximate
281 strength curve, it is then possible to determine the age or maturity at which a given concrete mix
282 achieves a target strength, or another specified performance metric. Using predefined strength gain
283 history curves which allow the user to approximate the instantaneous compressive or flexural
284 strength will likely minimize the extent of mechanical testing of hardened concrete specimens
285 during the early-age period. Once the user interpolates the age at which the target concrete strength

286 is expected to manifest, destructive mechanical testing of cylinders and/or plain concrete beams
287 can then serve to verify the strength performance as opposed to relying on multiple laboratory tests
288 throughout the anticipated early-age window. This information can then facilitate removal of
289 hardened HVFA components from formwork and more broadly contribute to optimizing turnover
290 of casting beds. Moreover, the outcomes of this approach will help to streamline the process for
291 informed estimation of elastic region concrete behavior at critical points like lifting/handling, and
292 supports integration of higher replacement values of SCMs in precast applications with stringent
293 early-age strength requirements. All approaches herein provide an approximation for concrete
294 cracking moment within the 24 hour early-age window, which is generally the most critical time
295 period for precast facilities as discussed previously.

296 Figure 4 presents a graphical description of the proposed framework and the three threads,
297 each with varying fidelity and complexity from which the user can choose to estimate the early-
298 age cracking moment. The framework was originally developed in a laboratory where ambient
299 conditions and basic equipment emulative those found in a precast facility. Therefore, the steps
300 outlined in Figure 4 can also be applied in a realistic precast environment where access to relevant
301 testing resources and equipment is also available. The process of extrapolating material properties
302 for use with larger-scale precast component is fairly standard, however, the novel pathways and
303 their associated design recommends are meant to further enhance precast productivity without
304 neglecting pertinent structural limit states in the early-age window. Thread I utilizes an age-
305 dependent procedure, whereas Thread II incorporates maturity measurements to account for the
306 internal temperature of the concrete. Thread III relies on direct testing of modulus of rupture, if
307 feasible for the user. The three main rows provide the critical steps needed to calculate the cracking
308 moment for each thread. These steps first include correlating compressive strength to time or

309 maturity, then calculating modulus of rupture from relationships with the corresponding
310 compressive strength or direct testing, and finally calculating the cracking moment of a concrete
311 section with the obtained modulus of rupture. The main advantage of using this framework comes
312 from allowing the user to select the best thread for a given application, the resources available
313 (e.g., testing equipment, maturity sensors, etc.), and the intended fabrication and curing conditions.
314 Thread I is likely the simplest to implement as it does not require maturity sensors and is the most
315 familiar with standard practice of calculating the cracking moment. Thread II is likely more
316 advantageous with variable curing conditions or when maturity sensors are already being used on
317 a given job to track strength development. Thread III is the most straightforward but will likely
318 require more laboratory work as it lacks a correlation with time or maturity to approximate strength
319 rather than performing multiple rounds of testing on plain concrete beam samples. Towards the
320 end of this paper, the accuracy of each thread will be demonstrated in conjunction with
321 experimental test results for HVFA concrete beams and the outcomes will provide additional
322 insight when choosing which thread to use for a given case. It should be noted that the experimental
323 validation step (i.e., the fourth row as shown in Figure 4) will likely not be feasible for the user
324 and was added in this study to demonstrate the effectiveness of the proposed framework. Large-
325 scale structural testing conducted to fulfill the optional fourth row in the framework (see Figure 4)
326 can be to provide validation of the three pathways for the user with their specific types of
327 components or applications. A case study will provide an example test program to provide data for
328 the purposes of this fourth row will be presented in Section 3.4 of this paper.



329

330

331

Figure 4 – Flowchart showing proposed multi-dimensional cracking moment calculation

framework

332

3.1. Thread I: Cracking Moment via Age-Dependent Strength

333

334

335

336

337

338

339

The results outlined in this thread were used to determine compressive, and ultimately flexural strength, with respect to concrete age. The steps outlined in Section 2 to produce the compressive strength versus concrete age relationship, like the examples done for this paper shown in Figure 1, should first be followed. Laboratory modulus of rupture tests done at the same age as the cylinder tests will then facilitate correlations with the square root of the corresponding compressive strength, as was done in Figure 3 and Equation 14-Equation 17 for demonstration purposes in this paper. Thread I also provides the option to bypass modulus of rupture testing (if

340 equipment is not available for example) and instead use Equation 2 to calculate it from
341 compressive strength (with expectedly less accuracy). The cracking moment capacity can then be
342 calculated using Equation 1 which will indirectly correlate it back to concrete age. The user can
343 then determine the concrete age (via back-calculation in the relationship plot) at which the
344 estimated cracking moment capacity exceeds the maximum moment demand expected during
345 lifting of the component to ensure the member remains uncracked (especially for Class U
346 prestressed members). The user may elect to impose a safety margin to ensure the cracking moment
347 capacity remains comfortably higher than the corresponding moment demand. Select precast
348 and/or prestressed members may necessitate stress checks during lifting and handling and in such
349 applications, comparisons between modulus of rupture calculated using Thread I or Thread II (see
350 below) and the tensile stress demand may substitute for the cracking moment check.

351 ***3.2. Thread II: Cracking Moment via Maturity-Dependent Strength***

352 Similar to Thread I (see Section 3.1) with the exception of now using temperature sensors,
353 the steps outlined in Section 2 should be followed to construct the compressive strength versus
354 concrete maturity relationship, like in the examples done for this paper as shown in Figure 2. The
355 approach to calculate modulus of rupture and subsequently the cracking moment for a given
356 section is then the same as discussed in Thread I. The maturity corresponding to the desired
357 cracking moment capacity can then be back-calculated to arrive at the target maturity value to
358 commence lifting/handling. That target value can then be checked against the data acquired from
359 a wireless temperature sensor (the same one used to determine the concrete maturity values during
360 preliminary testing should be used to eliminate any sources of error between sensor models)
361 installed in the member and activated prior to concrete placement in the precast plant.

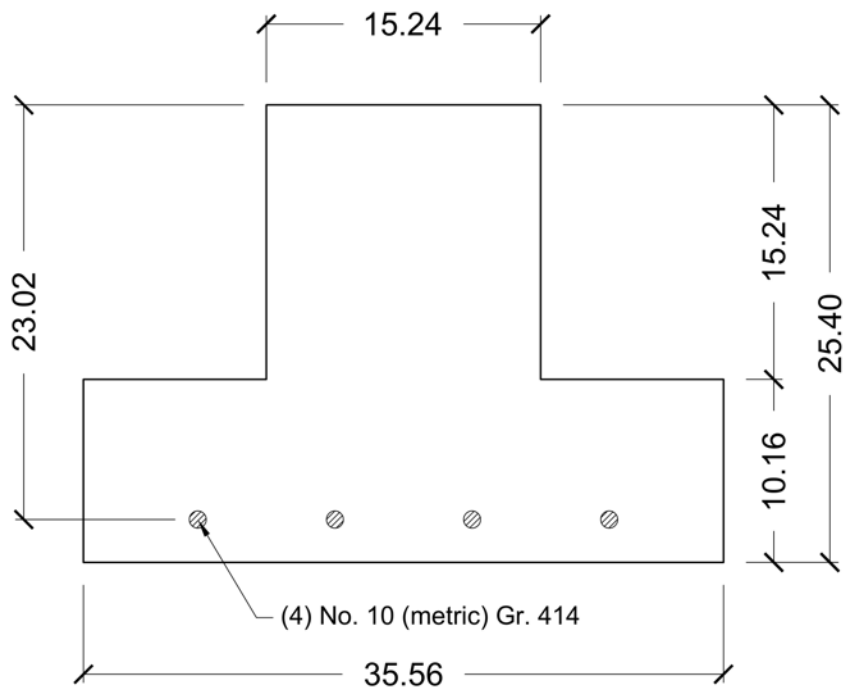
362 **3.3. Thread III: Cracking Moment via Direct Modulus of Rupture Testing**

363 The third thread likely will facilitate the most straightforward prediction of the cracking
364 moment as it relies on direct modulus of rupture testing (in accordance with ASTM C78 [4]) to
365 commence lifting/handling. It may, however, be more difficult to implement unless the laboratory
366 at a given precast facility has the equipment and complementary instrumentation needed to
367 perform the test. If this option is selected, it is important that plain concrete beams for modulus of
368 rupture testing be subjected to a curing environment that emulates the conditions exposed to the
369 precast member in the casting beds. For the purposes of this study, this third thread will largely
370 serve as an auxiliary comparison to the first two threads due to its independence of relationships
371 between modulus of rupture and the corresponding compressive strength.

372 **3.4. Validation with Experimental Beam Test Data**

373 In order to validate the streamlined framework proposed herein for estimating early-age
374 cracking moment capacity, a half-scale inverted tee section with dimensions as shown in Figure 5
375 (reference section is 28IT20 from the PCI Design Handbook [21]) with an overall length of 3.35
376 m (11 ft.) was cast from each fly ash mix examined for age- and maturity-dependent strength
377 development (i.e., *C40-G-NCA*, *F40-SHA*, and *L40-G-CI* as presented in Ordillas et al. [19]). The
378 members were loaded in three-point bending with simple supports and a span length of 3.1 m (10
379 ft.) using a large-format universal testing machine – a photo showing the complete test setup is
380 shown in Figure 6. During the test, the crosshead, to which a steel roller was mounted to simulate
381 a point load, is locked while the bottom platform, on which the two supports rest, is raised using
382 an automatic displacement-controlled profile. Force was recorded using a pancake load cell bolted
383 directly above the center steel roller and midspan deflection was acquired using a string
384 potentiometer mounted to the test frame below the beam.

385 The age and maturity of the concrete was recorded at the onset of each test, and the applied
386 moment at which cracking occurred was compared to the predicted cracking moment of the section
387 using the three threads presented in Sections 3.1 through 3.3. Table 1 provides the age and
388 corresponding maturity of the concrete for each beam test, which were selected such that the
389 expected cracking moment exceeded the maximum lifting/handling induced (i.e., self-weight)
390 moment by a factor of at least 6. This decision was made to ensure premature cracking did not
391 occur during lifting/handling, since the members were prefabricated in the lab, and consequently
392 compromise the safety of the researchers. Additionally, realistic precast members with relatively
393 larger span to depth ratios will crack at significantly less applied force for a given modulus of
394 rupture which justifies using a higher factor in the testing program. Note that the maturity values
395 recorded in Table 1 were obtained at the time of the test from wireless temperature sensors with a
396 probe embedded in the beams. Table 1 also shows the average experimental modulus of rupture at
397 the time of each beam test which is needed for Thread III of the framework.



398

399 Figure 5 – Inverted tee beam cross-section used in experimental tests (length dimensions in cm)



400

401 Figure 6 – Photo of an experimental HVFA inverted tee beam installed in the test setup

402

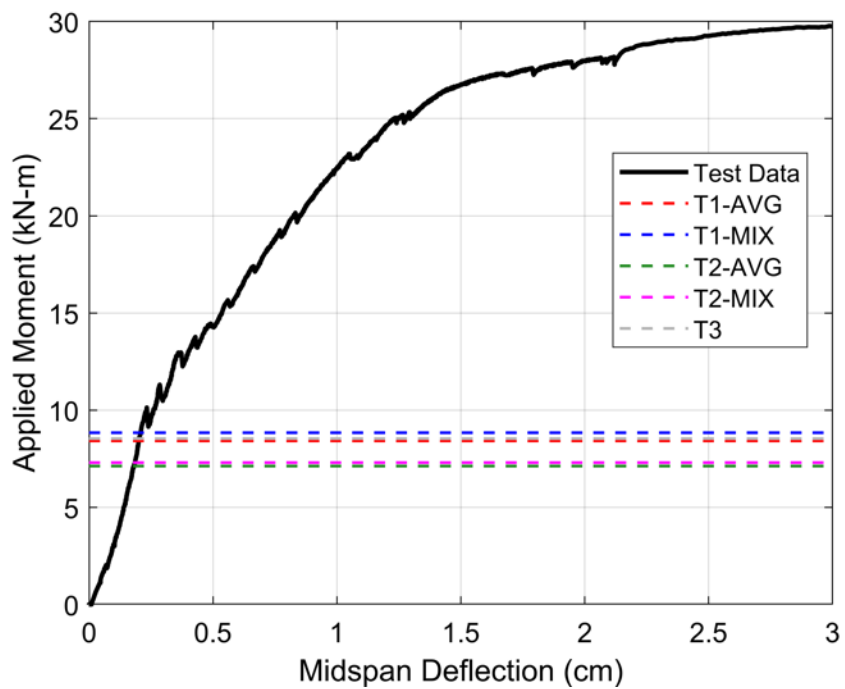
Table 1 – Average mechanical testing results and timeframes corresponding to beam tests

Beam ID	Mix ID (see Ordillas et al [19])	Age at Test (hrs)	Maturity at Test (°C-hrs)	f_r (MPa)
C	C40-G-NCA	17	358	3.61
L	L40-G-CI	16.5	507	3.95
F	F40-SHA	16.75	528	3.85

403

404 Figure 7-9 present plots of applied moment versus midspan deflection derived from
 405 experimental test data for beams C, L, and F, respectively. Also plotted in these three figures are
 406 the estimated cracking moment values as tabulated in Table 2 which were obtained using the three
 407 threads of the framework proposed in Sections 3.1 through 3.3. For Threads I ($T1$) and II ($T2$), two
 408 values were calculated – one using the average (*AVG*) fit equations across all fly ash types (see
 409 Equation 9, 13, and 17) and the other using the mix-specific (*MIX*) equation (see Equation 6-8, 10-
 410 12, and 14-16). Note that the *Experimental M_{cr}* value from each test was approximated graphically
 411 as the point where the *Test Data* curve first deviated from its linear-elastic region (i.e., the
 412 approximate proportional limit) via monitoring of the tangent stiffness. Figures 7-9 show that the
 413 cracking moment capacity estimates are conservative with respect to the corresponding
 414 experimental test result for each of the three beams, albeit less conservative than using Equation 2
 415 to calculate the modulus of rupture since its coefficient (i.e., 0.623) is less than those of Equation
 416 14-17 used to develop these figures. Therefore, while Equation 2 may facilitate a more
 417 conservative design, the implementation of Equation 14-17 will facilitate more accurate,
 418 performance-driven estimates of early-age cracking moment performance with beneficial
 419 applications for the fabrication of precast components. Furthermore, even with the higher
 420 coefficients proposed to calculate modulus of rupture, a comfortable margin of safety remains
 421 between the estimated cracking moment values and the actual results determined from

422 experimental testing. This observation may help to overcome some reservations about using a less
 423 conservative, performance-driven equation in place of the more established Equation 2. As for
 424 assessing the relative effectiveness of the three framework threads, Table 2 highlights that the
 425 majority of cases exhibited error percentage magnitudes of 25% or less. Thread III (*T3*), developed
 426 to be the most straightforward comparison between modulus of rupture and cracking moment, did
 427 not produce the most accurate result for any of the three beam cases. Generally, the age-dependent
 428 approaches performed well for beam C and the maturity-dependent calculations demonstrated the
 429 best performance for beams L and F. These results reinforce the importance of thoroughly
 430 evaluating a given mix design while scaling up its use for precast structural components and
 431 motivates the use of the framework developed herein to facilitate more accurate and
 432 comprehensive assessments of early-age cracking moment performance.



433
 434 Figure 7 – Experimental moment versus midspan deflection results for beam C along with
 435 estimated cracking moment values

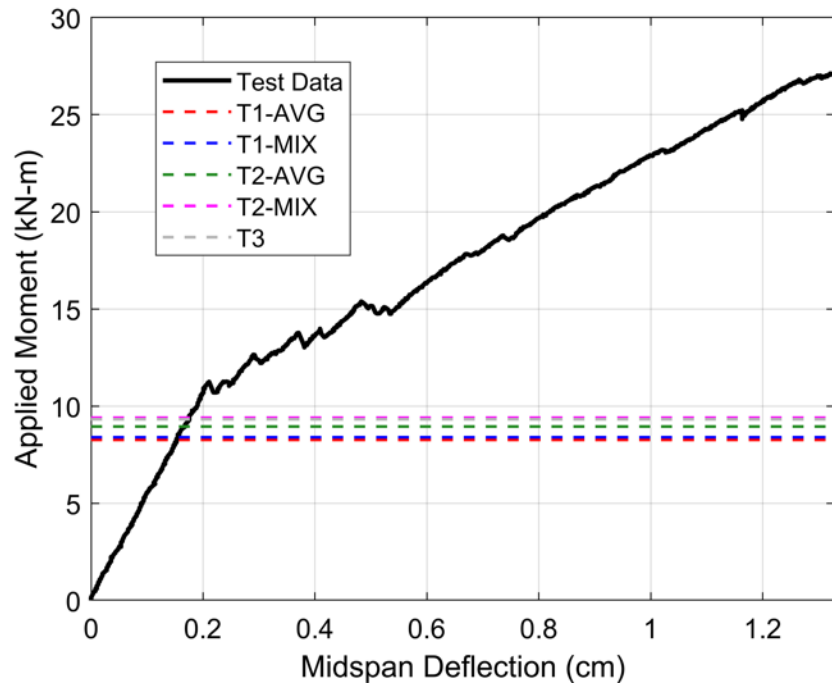
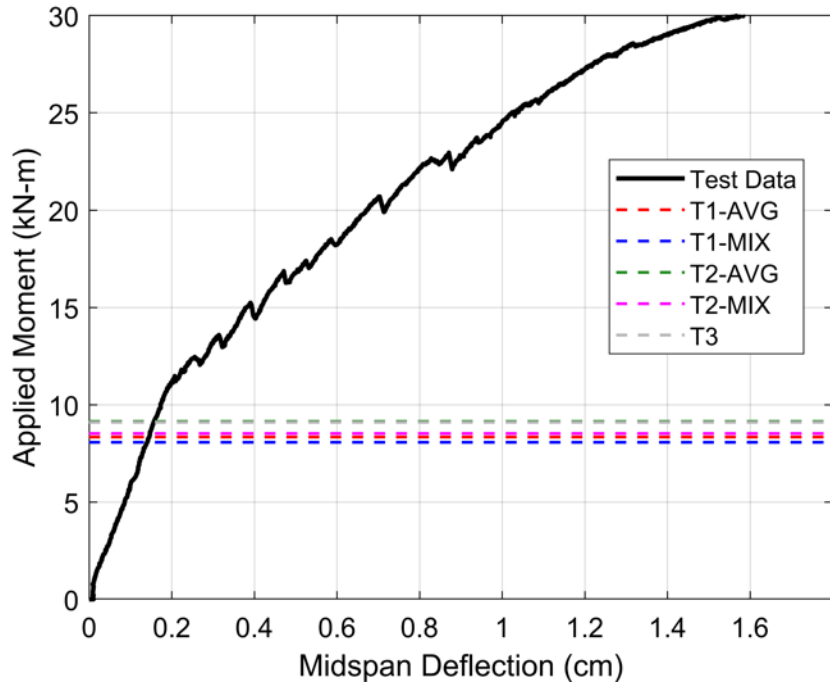


Figure 8 – Experimental moment versus midspan deflection results for beam L along with estimated cracking moment values



440
441 Figure 9 – Experimental moment versus midspan deflection results for beam F along with
442 estimated cracking moment values

443 Table 2 – Estimates of cracking moment capacity for each beam using the three framework
444 threads

Beam ID	C	L	F
Experimental M_{cr} [kN-m]	10.13	11.22	11.15
Average Fit Thread I M_{cr} [kN-m]*	8.42 (-16.9 %)	8.26 (-26.4 %)	8.34 (-25.2 %)
Mix Fit Thread I M_{cr} [kN-m]*	8.84 (-12.8 %)	8.39 (-25.2 %)	8.07 (-27.7 %)
Average Fit Thread II M_{cr} [kN-m]*	7.12 (-29.8 %)	8.95 (-20.2 %)	9.14 (-18.0 %)
Mix Fit Thread II M_{cr} [kN-m]*	7.30 (-28.0 %)	9.40 (-16.2 %)	8.52 (-23.6 %)
Thread III M_{cr} [kN-m]*	8.53 (-15.8 %)	9.32 (-16.9 %)	9.10 (-18.4 %)

445 *Note: Error % relative to Experimental M_{cr} value is show in parentheses in subsequent rows.
446

447 **4. SUMMARY AND CONCLUSIONS**

448 This paper proposed a multi-faceted framework structured to improve the accuracy of
449 calculating early-age flexural strength of precast components fabricated using high-volume fly ash
450 concrete mixes. The framework contains three threads (or options) from which the user can select
451 depending on the application or resources available to them. The first thread estimates the cracking
452 moment of a structural concrete beam simply as a function of the age of the concrete whereas the
453 second thread relies on measurements of concrete maturity as a more sophisticated indicator of
454 concrete strength development. Lastly, the third thread is theoretically the most straightforward as
455 it relies on direct modulus of rupture testing at the time when cracking moment is to be calculated,
456 rather than using a strength gain model. Traditional correlations between modulus of rupture and
457 the square root of the corresponding compressive strength have been reassessed for high early
458 strength concretes with high fractions of Portland cement replacement with fly ash. Additionally,
459 this performance was evaluated under the influence of ambient curing conditions which emulate
460 the environment of a typical precast facility. A series of experimental tests on concrete beams
461 prefabricated in a laboratory setting emulative of a precast facility helped to further demonstrate
462 scalability of the HVFA mix designs used in this study and also served to produce data for
463 validation of the proposed framework. More specifically, the following primary conclusions can
464 be drawn based on the research performed in this study:

465 ▪ Straightforward log-based equations were proposed to approximate early-age compressive
466 strength as a function of concrete age or maturity, from which modulus of rupture can then
467 be calculated. Using compressive strength as the starting point for Threads I and II aims to
468 facilitate ease of implementation for these approaches as cylinder tests are typically most
469 convenient and straightforward to run in the materials laboratory at a precast facility.

470 ▪ The proposed framework leads to improved accuracy when calculating the modulus of
471 rupture as a function of the square root of the compressive strength. Whereas ACI 318-19
472 Equation 19.2.3.1 uses a coefficient of 0.623, the values determined in this study range
473 from 0.686 to 0.787. Experimental tests of prefabricated concrete beams showed the new
474 coefficients still facilitate safe estimates of cracking moment despite their inherently less
475 conservative nature.

476 ▪ Estimates of cracking moment were within 25% of their corresponding experimental test
477 result in the majority of cases examined in this paper. While arguably the most
478 straightforward approach, Thread III was not the most accurate method with any of the
479 three beam tests.

480 ▪ The concrete age-based Thread I was most accurate for the fresh Class C fly ash beam,
481 coming within 12.8% of the experimental cracking moment in that case. The maturity-
482 based Thread II was most accurate for the landfilled and fresh Class F fly ash beams, with
483 error percentages of 16.2% and 18.0%, respectively.

484 ▪ Average fitting equations developed using the total breadth of data for all three fly ash
485 types were generally less accurate, relative to those proposed for each fly ash type
486 separately, in estimating cracking moment, except for the fresh Class F fly ash beam.

487 **5. ACKNOWLEDGEMENTS**

488 This material is based upon work supported by the Department of Energy under Award
489 Number DE-FE0031931. This publication was prepared as an account of work sponsored by an
490 agency of the United States Government. Neither the United States Government nor any agency
491 thereof, nor any of their employees, makes any warranty, express or implied, or assumes any legal
492 liability or responsibility for the accuracy, completeness, or usefulness of any information,

493 apparatus, product, or process disclosed, or represents that its use would not infringe privately
494 owned rights. Reference herein to any specific commercial product, process, or service by trade
495 name, trademark, manufacturer, or otherwise does not necessarily constitute or imply its
496 endorsement, recommendation, or favoring by the United States Government or any agency
497 thereof. The views and opinions of authors expressed herein do not necessarily state or reflect
498 those of the United States Government or any agency thereof.

499 **6. REFERENCES**

500 [1] A.K. Krishnan, Y.C. Wong, Z. Zhang, A. Arulrajah, A transition towards circular economy
501 with the utilisation of recycled fly ash and waste materials in clay, concrete and fly ash
502 bricks: A review, *Journal of Building Engineering* 98 (2024) 111210.
503 <https://doi.org/10.1016/j.jobe.2024.111210>.

504 [2] M. Meera, S. Gupta, Performance evaluation of marble powder and fly ash concrete for
505 non-structural applications, *Journal of Building Engineering* 84 (2024) 108499.
506 <https://doi.org/10.1016/j.jobe.2024.108499>.

507 [3] ACI Committee 318, ACI 318-19 Building Code Requirement for Structural Concrete and
508 Commentary, American Concrete Institute, Farmington Hills, MI, 2019.

509 [4] ASTM International, ASTM C78-22 Standard Test Method for Flexural Strength of
510 Concrete (Using Simple Beam with Third-Point Loading), ASTM International, 2022.

511 [5] F. O Slate, A.H. Nilson, S. Martinez, Mechanical Properties of High-Strength Lightweight
512 Concrete, *ACI Journal* (1986).
513 <https://www.concrete.org/publications/internationalconcreteabstractsportal.aspx?m=details&id=10454> (accessed June 18, 2024).

515 [6] D. Geng, N. Dai, X. Jin, E. Miao, Comparison of calculating methods and applications of
516 different concrete maturity, *Journal of Physics: Conference Series* 2011 (2021) 012022.
517 <https://doi.org/10.1088/1742-6596/2011/1/012022>.

518 [7] ASTM International, ASTM C1074-19e1 Standard Practice for Estimating Concrete
519 Strength by the Maturity Method, ASTM International, 2021.

520 [8] ASTM International, ASTM C918-20 Standard Test Method for Measuring Early-Age
521 Compressive Strength and Projecting Later-Age Strength, ASTM International, 2020.

522 [9] Giatec Scientific Inc., Concrete Maturity Calculation Methods, Giatec Scientific Inc.
523 (2019). <https://www.giatecscientific.com/education/concrete-maturity-calculation-methods/>
524 (accessed October 23, 2023).

525 [10] L. Wang, H. Zhou, J. Zhang, Z. Wang, L. Zhang, M. Nehdi, Prediction of concrete strength
526 considering thermal damage using a modified strength-maturity model, *Construction and*
527 *Building Materials* 400 (2023). <https://doi.org/10.1016/j.conbuildmat.2023.132779>.

528 [11] A. Mahmood, I. Hampton, Strength-maturity relationship of BCSA cement concrete, 49
529 (2023) 44–51.

530 [12] B.H. Tekle, S. Al-Deen, M. Anwar-Us-Saadat, N. Willans, Y. Zhang, C.K. Lee, Use of
531 maturity method to estimate early age compressive strength of slab in cold weather,
532 Structural Concrete 23 (2022) 1176–1190.

533 [13] A.M. Kaburu, J.W. Kaluli, C.K. Kabubo, Use of the Maturity Method in Quality Control of
534 Concrete: A Review, in: Proceedings of the Sustainable Research and Innovation
535 Conference, 2022.

536 [14] F. Kanavaris, M. Soutsos, Applicability of the Modified Nurse-Saul (MNS) maturity
537 function for estimating the effect of temperature on the compressive strength of GGBS
538 concretes, Construction and Building Materials 381 (2023).
539 <https://doi.org/10.1016/j.conbuildmat.2023.131250>.

540 [15] L. Hrishev, I. Rostovsky, I. Conev, V. Nikolov, Investigation for estimating of concrete
541 strength by the maturity method and the rebound hammer test, (2022) 40001.
542 <https://doi.org/10.1063/5.0104091>.

543 [16] S. Kazemifard, S. Motaghed, N. Eftekhari, NDT prediction of self-compacting concrete
544 strength based on maturity method, 2022. <https://doi.org/10.21203/rs.3.rs-2424241/v1>.

545 [17] M. Maraşlı, S. Guntepe, V. Ozdal, B. Kohen, H. Dehghanpour, S. Subaşı, Development of
546 Maturity Measurement Method and Device in Glass Fiber Reinforced Concrete (GRC),
547 2023.

548 [18] ASTM International, ASTM C511-21 Standard Specification for Mixing Rooms, Moist
549 Cabinets, Moist Rooms, and Water Storage Tanks Used in the Testing of Hydraulic
550 Cements and Concretes, (2021).

551 [19] K.A. Ordillas, M.J. Gombeda, F. Mendonca, Z.N. Lallas, Reassessing early-age strength
552 development of high-volume fly ash concretes for precast buildings, Journal of Building
553 Engineering 100 (2025) 111630. <https://doi.org/10.1016/j.jobe.2024.111630>.

554 [20] ASTM International, ASTM C39-24 Standard Test Method for Compressive Strength of
555 Cylindrical Concrete Specimens, ASTM International, 2024.
556 https://doi.org/10.1520/A0996_A0996M-16.

557 [21] Precast/Prestressed Concrete Institute, MNL120-17 - PCI Design Handbook, 8th Edition,
558 Chicago, IL, 2021.

559